International Journal of Disaster Risk Reduction 137 (2026) 106105

Contents lists available at ScienceDirect

International Journal of Disaster Risk Reduction

journal homepage: www.elsevier.com/locate/ijdrr

An assessment of aerial firefighting response times between agencies during the 2020 fire season in California

Shayne Magstadt [a,*], Erin J. Belval [b], Bradley M. Pietruszka [c], Yu Wei [a], Christopher D. O'Connor [d]

[a] Department of Forest and Rangeland Stewardship, Colorado State University, 1472 Campus Delivery, Fort Collins, CO, 80523, USA
[b] Human Dimensions Science Program, Rocky Mountain Research Station, USDA Forest Service, Fort Collins, CO, 80526, USA
[c] Human Dimensions Program, Rocky Mountain Research Station, USDA Forest Service, 240 W Prospect Road, Fort Collins, CO, 80526, USA
[d] United States Department of Agriculture, Forest Service, Rocky Mountain Research Station, 800 East Beckwith Avenue, Missoula, MT, 59801, USA

A B S T R A C T

Rapid, well-coordinated aerial response can limit wildfire growth during the initial response (IR) period. Most quantitative studies of wildland fire aviation effectiveness have relied on aircraft data from the United States Forest Service (USFS), with comparatively less attention to other agencies. This study leverages open ADS-B data to reconstruct second-by-second aircraft movements for both the California Department of Forestry and Fire Protection (CAL FIRE) and USFS fleets during the 2020 California fire season, enabling the first direct cross-agency comparison of operational use. We characterize fleet activity patterns and evaluate how landscape, weather, and values at risk influence time to first aircraft arrival within 24 h of ignition. ADS-B flight tracks were matched to 7214 wildfires; response time was defined as the interval between ignition discovery and the first ADS-B detection within 5 km. Cause-specific cumulative incidence curves compared the probability that each agency arrived first. Cox proportional hazards models, stratified by diurnal period and protecting agency, quantified the effects of slope, fuel moisture, temperature, distance to water, and human exposure metrics on dispatch timing. Aircraft responded to 1476 fires, with USFS aircraft exhibiting slightly shorter mean response times. Hazard ratios indicated faster response under higher temperatures and closer proximity to populated areas, whereas wetter fuels and greener-than-average vegetation were associated with delayed arrival. These results demonstrate the feasibility of near–real-time, cross-agency performance monitoring to inform resource allocation and support integration of ADS-B data with federal tracking systems for enhanced aviation situational awareness.

1. Introduction

Wildland firefighting agencies employ a diverse array of strategies and resources to combat wildfires, including the extensive use of aviation assets. Aerial resources, such as helicopters and air tankers, influence fire outcomes by delivering water, retardant, and personnel to locations in difficult terrain or areas with limited water access, while also providing critical intelligence to support decision-making on the ground. In California, two prominent agencies, the USFS and CAL FIRE, manage significant aviation operations designed for wildfire response. Although CAL FIRE and the USFS are distinct organizations shaped by different mandates and missions, they are united by a shared responsibility for wildfire suppression and have legal agreements to work in coordination, particularly during the IR phase when aviation resources are rapidly mobilized [1,2]. CAL FIRE and the USFS operate under reciprocal Direct Protection Area (DPA) arrangements in California, whereby either agency may hold primary suppression responsibility on state or federal lands, including some areas under federal jurisdiction [3]. Additionally, Region 5 of the USFS (which is comprised of the state of California) accounted for nearly a quarter of all aviation flight hours contracted by the agency, further illustrating the high use of

* Corresponding author.
E-mail address: Shayne.Magstadt@colostate.edu (S. Magstadt).

https://doi.org/10.1016/j.ijdrr.2026.106105
Received 7 January 2026; Received in revised form 3 March 2026; Accepted 16 March 2026
Available online 16 March 2026
2212-4209/© 2026 Published by Elsevier Ltd. This is an open access article under the CC BY-NC-ND license (http://creativecommons.org/licenses/by-nc-nd/4.0/).

aerial firefighting support in California [4].

During the IR phase of wildfire response, both CAL FIRE and the USFS prioritize rapid aircraft dispatch using the *closest resource concept*, ensuring the nearest available aircraft responds to a fire regardless of agency ownership National Interagency Coordination Center [5]. This cooperative approach enables the efficient use of limited aerial suppression assets across overlapping jurisdictions, particularly in California where state and federal responsibilities frequently intersect. Wildfire managers directly order aircraft from the administering airbase via intercom if the base is staffed; otherwise, they place requests through the Geographic Area Coordination Center (GACC), which manages aircraft availability and assignment statewide.

The importance of this coordinated aerial response became especially evident during California's 2020 wildfire season, one of the most destructive and costly on record [6]. Firefighting agencies in California responded to 8648 wildfires, which collectively burned more than 4.3 million acres across the state, more than double the recent previous state-record and representing nearly 4% of California's land area [7]. Among these, the August Complex Fire became California's first officially recognized *gigafire*, burning more than 1 million acres across seven counties [8]. The exceptional scale and intensity of these incidents placed demands on aerial resources, prompting both CAL FIRE and the USFS to heavily utilize aircraft to support suppression efforts across the state.

To meet these demands, CAL FIRE operates the largest civil aerial firefighting fleet in the world, as a component of its wildfire suppression program. The agency's aviation program includes a diverse array of aircraft designed to deliver rapid fire suppression in California's challenging and often extreme wildfire conditions. CAL FIRE manages its fleet of approximately 24 tankers, 25 helicopters, and 19 tactical aircraft from 14 strategically located air tanker bases across the state [2]. In comparison, Region 5 (California) accounted for the highest level of Forest Service aviation activity nationwide, with 20,550 flight hours, representing 24.7% of all Forest Service aviation use and more than double any other region [4]. The regional fleet included a mix of contracted and agency-owned helicopters, fixed-wing aircraft, airtankers, and water scoopers that supported wildfire suppression and other mission needs. Of these, helicopters played a particularly critical role, reflecting the region's reliance on rapid aerial suppression in steep and inaccessible terrain. Across the Forest Service, aircraft delivered over 122 million gallons of liquid, of which more than 119 million gallons were water and 3.4 million gallons were retardant, with a significant share occurring in California due to the region's extensive fire activity. Region 5 airtanker operations totaled approximately 1616 flight hours (17.1% of national airtanker time). Currently, the USFS tracks the application of these liquids using Automated Telemetry Unit (ATU) to document resource use [9]; however, comparable data for CAL FIRE operations are not publicly available, limiting direct comparisons between federal and state aerial suppression metrics.

No unified aviation dataset exists that captures cross-agency aircraft activity during wildfire response, preventing evaluation of statewide IR coordination. This lack of publicly accessible state-level aviation data underscores the value of leveraging independent, standardized tracking systems. Automatic Dependent Surveillance–Broadcast (ADS-B) technology, already mandated across most U.S. airspace, offers a solution by providing continuous, high-resolution data on aircraft location and movement [10–12]. Federal Aviation Administration (FAA) regulations mandate the use of ADS-B Out transmitters in most airspaces, enabling the monitoring of firefighting aircraft [13]. ADS-B technology has been successfully integrated into wildland fire operations to monitor unmanned aircraft systems (UAS) [14,15]. It has also been used to analyze aerial firefighting operations, highlighting the effectiveness and cost-efficiency of different aircraft types based on mission patterns, deployment techniques, and resource delivery [16]. Because ADS-B is present on all aircraft and the reporting is standardized across agencies, ADS-B technology offers a valuable opportunity to enhance the tracking and analysis of aviation operations, providing insights into state-managed aviation resources that can complement existing research focused primarily on USFS operations.

The goal of this study is to use ADS-B flight tracking data and survival analysis techniques to quantify differences in IR response times, operational patterns, resource deployment strategies, and fleet usage between agencies involved in aviation operations in California in 2020. By applying Aalen-Johansen estimators and using Cox proportional hazards modeling approaches, the study seeks to generate empirical timelines of aircraft response times for these agencies during the IR phase. In addition to characterizing response patterns, the analysis will explore how physical, biological, social, and administrative attributes, such as topography, vegetation characteristics, and population density, influence the likelihood that a wildfire receives an aerial response during the first 24 h of ignition. Ultimately, the goal is to bridge methodological gaps between real-time aviation tracking and operational analysis, helping to inform more effective cross-agency coordination and aviation resource management strategies during wildfire suppression.

2. Methods and data

2.1. Data acquisition and fleet identification for CAL FIRE and USFS aircraft

This study uses ADS-B data provided by the OpenSky Network to address gaps in understanding aviation activities during wildfire suppression efforts [17]. The OpenSky Network is a non-profit organization that offers open access to real-world air traffic control data collected through a global network of ADS-B and Mode S sensors. By providing detailed flight trajectories, timestamps, and aircraft identifiers, OpenSky enables comprehensive analysis of aerial firefighting operations, including flight patterns and suppressant delivery activity [18,19].

To evaluate aerial operations conducted by CAL FIRE and the USFS during the 2020 California wildfire season, all known firefighting aircraft were identified by tail numbers and cross-referenced with Federal Aviation Administration (FAA) registration data to confirm aircraft make, model, and associated ADS-B identifiers [20]. ADS-B flight records for these aircraft were collected from the OpenSky Network using a Python-based workflow that automated monthly data retrieval via the *pyopensky* package and a *Trino* query interface [17,21]. Tail numbers were converted to their corresponding ICAO24 codes, which served as unique identifiers within the OpenSky database. Retrieved data were subsequently processed into GeoDataFrames for spatial and temporal analysis of aerial

suppression activity.

We accessed NASADEM tiles through the Planetary Computer STAC API [22], interpolated ground elevations at each aircraft location, and calculated height above ground level (AGL) by differencing geometric altitude from the surface elevation. Data were filtered to retain observations within a maximum 5000-m AGL threshold to focus on operational flight segments relevant to wildfire suppression. Finally, monthly outputs were saved as shapefiles to analyze temporal patterns, deployment behaviors, and survival

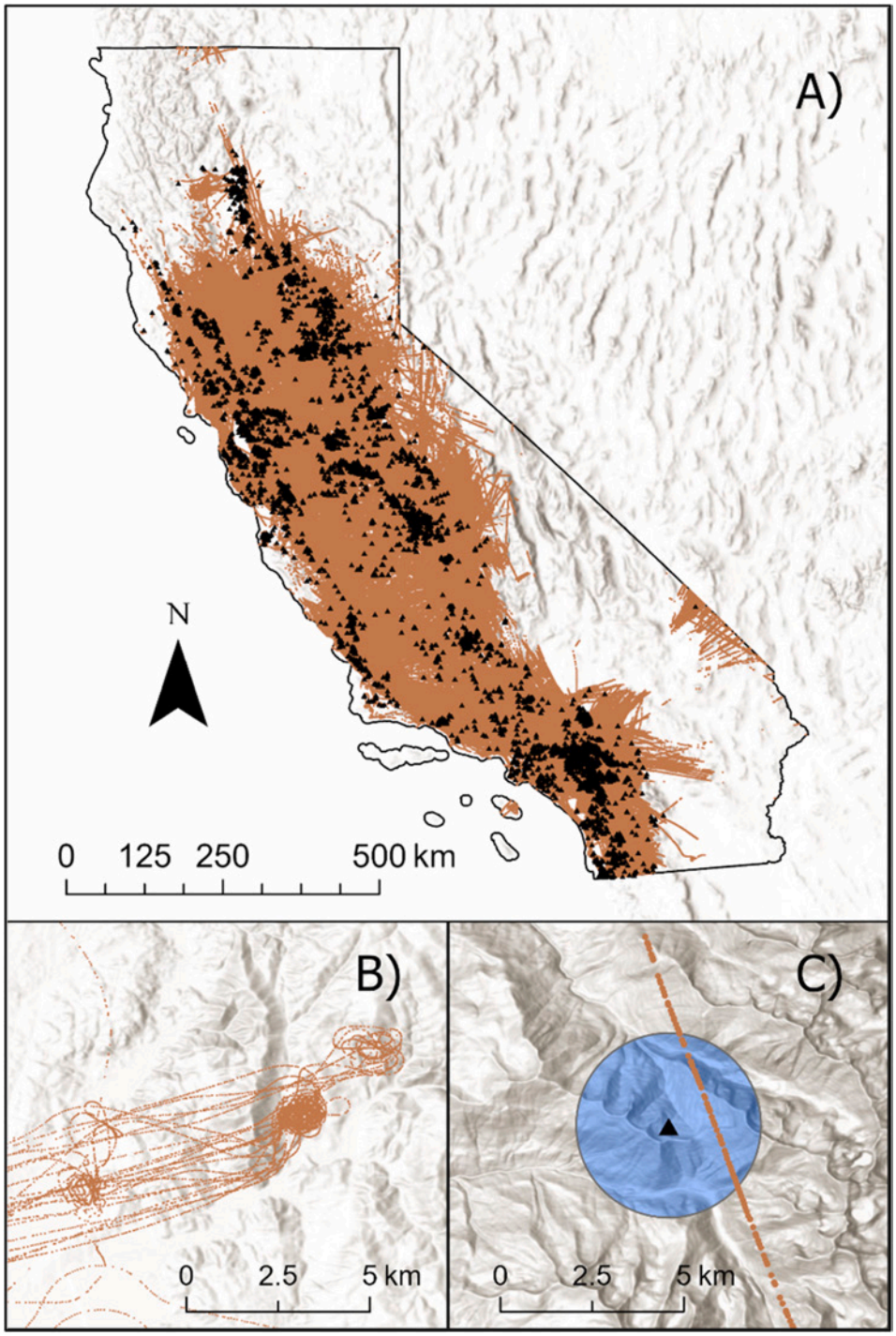

Fig. 1. An overview of the study area (A), including aircraft flight paths derived from ADS-B data in orange and wildfire ignition points represented as triangles across California. Insets illustrate (B) aircraft circling patterns near active fires and (C) the 5 km detection radius used to assess aircraft arrival after ignition.

Table 1
Summary of aircraft types and counts included in the ADS-B analysis for CAL FIRE and USFS aviation resources during the 2020 California fire season.

Agency	Aircraft Category	Aircraft Model	Count
CAL FIRE	Airtanker	Grumman S-2T	25
CAL FIRE	Airtanker	Lockheed C-130H Hercules	7
CAL FIRE	Helicopter	UH-1H Super Huey	12
CAL FIRE	Helicopter	Sikorsky S-70i	12
CAL FIRE	Tactical	Rockwell OV-10	18
CAL FIRE	Tactical	King Air A200	2
USFS	Very Large Airtanker (VLAT)	Multiple models	4
USFS	Large Airtanker (LAT)	Multiple models	48
USFS	Type 1 Helicopter	Multiple models	83
USFS	Type 2 Helicopter	Multiple models	42

modeling. This approach enabled the construction of a detailed, elevation-corrected movement dataset across both agencies' aviation operations. The dataset spans January 2020 through December 2020 and includes high-resolution positional information (latitude, longitude, altitude, and timestamp) recorded at a 1-Hz frequency (Fig. 1). Data coverage is based on the OpenSky Network's ground-based sensor network, which exhibits geographically variable coverage due to terrain and sensor distribution [23]. Because ADS-B reception relies on line-of-sight transmission to ground-based receivers, low-altitude aircraft operating in mountainous terrain may experience reduced detectability. This is particularly relevant in California, where CAL FIRE helicopters and airtankers frequently operate at low altitudes during suppression activities. Areas lacking nearby receivers or obstructed by terrain may therefore produce spatial gaps in ADS-B coverage. To reduce misclassification of non-detections as non-response, we excluded fires with no ADS-B detections within 5 km during 2020, thereby restricting analysis to the portion of the state observable through the OpenSky sensor network.

To examine CAL FIRE's aviation operations, the study focused on its permanently maintained, state-funded fleet, comprising 76 aircraft. As of 2025, this fleet included 25 Grumman S-2T airtankers, 7 Lockheed C-130H Hercules airtankers, 12 UH-1H Super Huey helicopters, 12 Sikorsky S-70i helicopters, 18 Rockwell OV-10 aircraft, and 2 King Air A200 aircraft [2]. A summary of aircraft types and counts included in this study is provided in Table 1. In contrast to CAL FIRE's permanent fleet model, the USFS relies on a dynamic combination of exclusive-use and call-when-needed contracts to secure its aerial firefighting resources. To focus specifically on aircraft capable of performing retardant drops, this study used ATU drop logs, which are required for all USFS-contracted aircraft capable of this operation, including airtankers and type one helicopters. Any aircraft that conducted at least one recorded retardant or water drop between 2017 and 2024 was included in the analysis. These aircraft were then cross-referenced with OpenSky ADS-B data to compile comprehensive flight histories. The USFS fleet identified in this dataset includes a range of helicopters and fixed-wing airtankers. Among the heavy-lift Type 1 helicopters, the most commonly used models included Boeing CH-47D, Sikorsky S-70i, Kaman K-1200, Sikorsky UH-60A, Sikorsky S-64E, and CH-54B helicopters. The mid-lift Type 2 helicopter fleet primarily included Bell UH-1H, Bell 205A-1, Airbus MBB-BK117 D-3, and Sikorsky S-58 variants. For fixed-wing airtankers, the USFS operated a variety of aircraft models including Bombardier DHC-8, Lockheed C-130, Boeing 737-3H4, McDonnell Douglas DC-9-87 and MD-87, British Aerospace AVRO 146-RJ85A and Bae 146, Bombardier CL-415, Canadair CL-215-6B11, and McDonnell Douglas DC-10. Overall, the USFS dataset captured four very large airtankers (VLATs), 48 large airtankers (LATs), 83 Type 1 helicopters, and 42 Type 2 helicopters actively engaged during the study period.

The USFS dataset covers helicopters and fixed-wing aircraft involved in wildfire suppression from 2017 to 2024, matching the full span of available ATU records. Because USFS helicopter ATU drop logs were anonymized, we did not have an exact year-by-year list of helicopters used; instead, we compiled a comprehensive 2017–2024 roster of USFS contracted aircraft and, for California, considered aircraft in-scope if they were wildland-mission capable, based in or regularly operating in the state, and had a plausible operational range for responding to California wildfires. Together with CAL FIRE, these datasets provide a detailed operational portrait of California's aerial firefighting and underpin our survival analyses.

2.2. Aviation use summary statistics

To complement the survival models, we developed a set of descriptive statistics that summarize aviation workload, response timing, and spatial deployment patterns for CAL FIRE and the USFS during the 2020 season. Using the full ADS-B dataset, we first calculated the number of unique active aircraft per day for each agency, producing a daily time series of fleet utilization. These daily activity profiles capture seasonal patterns in aircraft use and provide a baseline context for interpreting when each agency was most operationally engaged.

We then examined how proximity to airbases related to response outcomes by mapping all ignition points alongside airbase locations and classifying each fire by its first-arriving agency. For each ignition, we summarized response time metrics (mean, median, and percentile values), enabling a comparison of typical arrival times. Rather than relying solely on averages, we constructed empirical response-time distributions for both agencies to show how arrival times varied across the full IR window.

To assess spatial patterns of aviation activity, we rasterized all ADS-B flight trajectories to produce gridded density surfaces for CAL FIRE and USFS separately. Each raster records the cumulative number of aircraft-seconds per grid cell across the study period. We also generated a difference surface (CAL FIRE minus USFS), which highlights areas where one agency operated more intensively than the other. This product provides a spatially explicit view of how aircraft from each agency used airspace over the course of the season and supports comparisons of regional deployment patterns.

2.3. Aircraft response timing to initial fire discoveries

The OpenSky dataset provided timestamps, geographic positions, and unique aircraft identifiers (ICAO24 codes), which we processed to construct time series visualizations and to detect aircraft presence near wildfires. Wildfire occurrence data were obtained from the Fire Program Analysis Fire-Occurrence Database [24], which includes discovery date, discovery time (HHMM format), fire size, and ignition coordinates. Discovery is determined as the date and time recorded by the reporting agency when the fire was first detected or reported, typically based on initial observer report, dispatch logs, or incident documentation rather than the actual moment of ignition. Of the 10,198 wildfires reported in California in 2020, 8213 had valid discovery time and date information.

To calculate aviation response times, we spatially and temporally matched wildfire discovery records with ADS-B flight detections. Aircraft detections were filtered to those occurring within 5 km of a fire's ignition point and within 24 h following its discovery. The 5 km radius was selected to accommodate the positional uncertainty of ignition records, which are typically reported at section-level accuracy, ensuring that aircraft detections are captured even when discovery coordinates are offset from the true ignition location. We defined initial response as the first 24 h following discovery, consistent with federal guidance that treats this period as the typical length of the initial operational window before a fire transitions to extended response [25]. For each fire, response time was defined as the elapsed minutes between discovery and the first qualifying aircraft detection. As a sensitivity check, we repeated the analysis using alternative spatial thresholds of 7 km and 9 km; response time estimates were qualitatively similar across radii, indicating that results were not sensitive to the specific distance threshold chosen.

Fires with no recorded aircraft activity and no detections within this radius were excluded, as they likely occurred outside the effective surveillance range of the ADS-B network rather than reflecting a deliberate decision not to respond. This filtering step removed 1003 fires from the dataset and ensures that subsequent analyses reflect operational patterns within the ADS-B–observable portion of the state.

2.4. Initial response analysis

The data were structured so that each row represented a single response time observation per fire. The reshaped datasets were concatenated, and for each fire, the minimum recorded response time across both agencies was selected to define the duration to first aircraft arrival. Each fire was assigned an event code: one if CAL FIRE arrived first, two if USFS arrived first. Fires without a recorded response within the observation window were right-censored by setting their duration to the maximum observed time (24 h from fire discovery) and assigning an event code of zero.

The resulting dataset (FPA_ID, duration, event type, Agency) was then used to fit a nonparametric competing risks model using the Aalen–Johansen estimator [26]. For each unique event time, transition intensity matrices were constructed to represent the probability of transition into each of the two groups (CAL FIRE first, USFS first). These matrices were cumulatively multiplied to derive the cause-specific cumulative incidence functions (CIFs), which quantify the probability over time that each agency is the first to respond. CIFs were then plotted to visualize how these probabilities evolve, appropriately accounting for the competing nature of response events and censoring. Unlike standard survival curves, CIFs account for the fact that multiple outcomes can prevent the occurrence of one another, in this case, the arrival of one agency precludes the other from arriving first.

While the competing risks model identifies which agency is more likely to arrive first, it does not examine the factors influencing response timing. To study the influence of landscape, weather, and operational conditions on aircraft arrival, we applied a Cox proportional hazards model [27]. Using the same fire-level dataset, we kept each fire's observed duration and flagged the event indicator as 1 when an aircraft from either agency arrived and 0 when no aircraft arrived within 24 h. The model was fitted using the Breslow method for baseline hazard estimation and standard errors [28]. Estimated hazard ratios represent the multiplicative effect of each covariate on the instantaneous rate of aircraft arrival, holding other variables constant. Model fit and proportional hazards assumptions were assessed using the Schoenfeld residual-based diagnostics [29].

We estimated three separate Cox proportional hazards models. Each model incorporated the same covariates but differed in stratification approach. In the first model, we included no stratification to provide a baseline specification. The second model added fixed effects stratified by time of day, derived from the fire discovery time, based on prior evidence that large airtanker activity peaks during afternoon hours when fire behavior typically intensifies [30,31]. Fires were categorized into three periods based on local discovery hour: Morning (06:00–12:59), Afternoon (13:00–20:59), and Night (21:00–05:59). This classification allowed us to account for operational rhythms and diurnal variation in fire behavior and aircraft dispatch likelihood. The third model introduced stratification by DPA, which delineates zones of primary suppression responsibility across federal, state, and local fire agencies, to account for differences in fire management arrangements, resource availability, and dispatch practices across protection zones. This stratified modeling framework allowed us to evaluate the stability of covariate effects while accounting for temporal and jurisdictional heterogeneity in aerial response behavior.

Table 2
Covariate names, descriptions, and data sources used in the survival analysis of aerial initial response.

Variable Name	Description	Source
FM100	100-h dead fuel moisture (%)	[42]
NDVI anomaly	Standardized day-prior NDVI anomaly computed from four components (day-prior NDVI, and monthly mean, maximum, and minimum NDVI over the preceding 12 months)	[33, 46]
Slope	0-90°	[47]
Distance to water	Distance to nearest waterbody (km)	[48]
Wind speed	Wind velocity at 10 m above ground (m/s)	[42]
Burning Index	Burning Index (NFDRS fire danger index)	[42]
Max Temp °F	Maximum temperature	[42]
Global Human Mod	Cumulative measure of the human modification of lands within 1 km of the fire ignition point	[49]
Population	Average population density within a 1 km radius around the fire ignition point	[50]

2.5. Covariate selection

Vegetation and fuel characteristics have been shown to affect airtanker use and deployment patterns [32], making vegetation and fuel characteristics an important factor for modeling aerial suppression decisions. To characterize live fuel conditions consistently across California's diverse ecosystems, we used the Normalized Difference Vegetation Index (NDVI), which provides continuous spatial coverage and reflects live photosynthetic activity across forested, shrubland, grassland, and developed environments [33]. NDVI captures short-term variability in vegetation greenness that can influence ignition potential, flame intensity, and tactical considerations during the IR phase. Because vegetation stress typically appears as reduced greenness, negative NDVI anomalies, departures below a site's recent mean, have been linked to elevated wildfire potential [34–36].

We therefore derived a standardized day-prior NDVI anomaly for each fire using the following formulation:

$$NDVI_{ANOM} = \frac{NDVI_{d-1} - NDVI_{mean,m}}{\left(NDVI_{max,m} - NDVI_{min,m}\right)/4}$$

where $NDVI_{d-1}$ is the NDVI on the day before discovery, and $NDVI_{mean,m}$, $NDVI_{max,m}$, and $NDVI_{min,m}$ are the mean, maximum, and minimum NDVI values for the corresponding calendar month over the preceding 12 months. We scaled anomalies by dividing the month-specific NDVI range $\left(NDVI_{max,m} - NDVI_{min,m}\right)/4$, where the range is computed from the same calendar month over the preceding 12 months. This anomaly highlights departures from expected seasonal conditions, offering an indicator of live-fuel conditions that can shape how aircraft are used during initial response. Because unusually low NDVI anomalies signal stressed, more flammable live fuels, they also serve as a proxy for conditions under which initial response is more difficult to contain with ground resources.

To complement the live-fuel signal provided by NDVI, we included 100-h dead fuel moisture as a measure of background fuel aridity, a variable that strongly influences fire behavior and is a component of fire danger rating systems [37,38]. Lower dead-fuel moisture strongly influences fire behavior and increases the likelihood of ignition, rate of spread, and fireline intensity; 100-h fuel moisture is also an input to operational fire-behavior models, underscoring its importance [39].

Topographic constraints were represented using slope steepness from LANDFIRE terrain data. Steeper slopes can limit ground access, reduce handline effectiveness, and increase reliance on aerial resources [30,40]. Additionally, steep slopes tend to elevate firefighter risk by increasing flame exposure, entrapment potential, and the difficulty of safe escape route construction, conditions that often require greater suppression [41].

Weather-driven fire danger was characterized using wind speed, maximum temperature, and the Burning Index, all from GridMET [42]. These variables capture environmental conditions that are closely associated with periods of intensified fire behavior and increased demand for aerial support [30,40,43]. Because weather is one of the primary situational cues used by incident commanders, these factors are often incorporated, consciously or intuitively, into assessments of potential fire behavior and suppression needs [44]. Together, these weather variables provide a dynamic representation of conditions that influence both fire growth and the likelihood of early aircraft deployment.

Operational logistics were represented using distance to the nearest accessible surface water source, which serves as a proxy for potential dip-site availability and water resupply constraints during initial attack. In areas where suitable water bodies are distant, limited in size, or difficult to access due to terrain or infrastructure, aircraft and ground resources may experience longer turnaround times or reduced operational efficiency. Thus, greater distance to draftable water can represent a logistical constraint rather than simply a hydrologic characteristic of the landscape. Proximity to suitable water sources has been shown to influence both airtanker and helicopter deployment patterns [45], making this variable relevant for capturing spatial variation in suppression feasibility and response dynamics.

Finally, values-at-risk covariates were included to capture the influence of human exposure on aerial suppression decisions. The Global Human Modification Index and 1-km population density from WorldPop were used to represent development pressure and wildland–urban interface proximity, consistent with findings that aircraft deployments often concentrate near populated areas [32].

With the exception of distance to water sources, all covariates were sourced from the FPA FOD-Attributes dataset [33]. Table 2

provides the full list of variables, definitions, and data sources.

3. Results

3.1. Aircraft activity and seasonal patterns

We obtained 17,884,545 positional records (≈4968 flight hours) for USFS aircraft and 21,925,926 records (≈6090 h) for CAL FIRE aircraft, representing second-by-second tracking across the 2020 season where ADS-B data were available. CAL FIRE activity (Fig. 2, top) increased through the summer, peaked in September, and declined in November. USFS aircraft showed a broadly similar seasonal pattern but with a slightly later and more diffuse peak and fewer individual aircraft active on a typical day (Fig. 2, bottom).

To compare spatial patterns of airspace use, we generated a density-difference surface representing USFS aircraft density minus CAL FIRE aircraft density at a 3-km resolution (Figure A1). Positive values indicate areas more frequently traversed by USFS aircraft, while negative values indicate higher CAL FIRE activity. The map shows dense flight-path corridors and incident hubs across the state, with pockets of higher CAL FIRE activity indicated by dark purple values and pockets of higher USFS activity indicated by bright yellow values.

3.2. Incident summary and response times

A total of 7214 wildfire incidents were included in the analysis. Of these, 1476 received an aerial response within 24 h of discovery (840 CAL FIRE, 637 USFS), while 5737 had no recorded aerial response and were classified as "No Response." Response times were right-censored at 1440 min (24 h). Among incidents with a recorded response, CAL FIRE arrival times averaged 700 min (median 751; IQR: 387–1007), and USFS arrival times averaged 673 min (median 680; IQR: 406–962). Fifty-five incidents had an initial response within 20 min (37 CAL FIRE, 18 USFS).

3.3. Proximity to airbases

Distances from ignition points to the nearest CAL FIRE airbase ranged from about 0.25 to 254 km across all fires (Figure A2). Mean distances were 33.5 km for CAL FIRE-first responses (n = 840), 35.6 km for USFS-first responses (n = 637), and 46.9 km for No Response fires (n = 5737). Medians showed a similar pattern: 29.7 km (CAL FIRE-first), 35.4 km (USFS-first), and 42.7 km (No Response). Although the distributions overlapped across response types, fires that received an initial aerial response were generally closer to an airbase, while No Response fires exhibited both the largest mean and median distances.

Across all three panels in Fig. 3, ignition locations are distributed statewide with a broad north–south pattern along the Sierra Nevada, Coast Range, and southern California foothills. No Response fires (Panel A) are widely dispersed across the same areas where responded fires occur. CAL FIRE-first responses (Panel B) and USFS-first responses (Panel C) show overlapping geographic footprints, with both agencies' initial responses appearing throughout northern, central, and southern California. CAL FIRE airbases (triangles) are positioned across the state, and incidents of each response type occur in proximity to multiple bases rather than clustering around

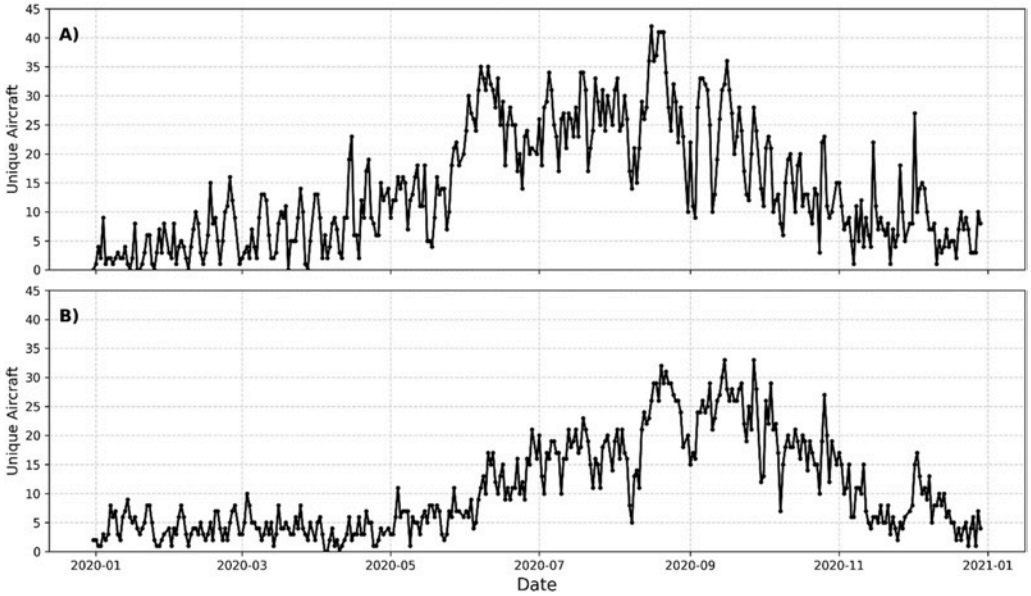

Fig. 2. Line plot illustrating the distribution of unique aircraft activities (CAL FIRE top, USFS bottom) by day for 2020.

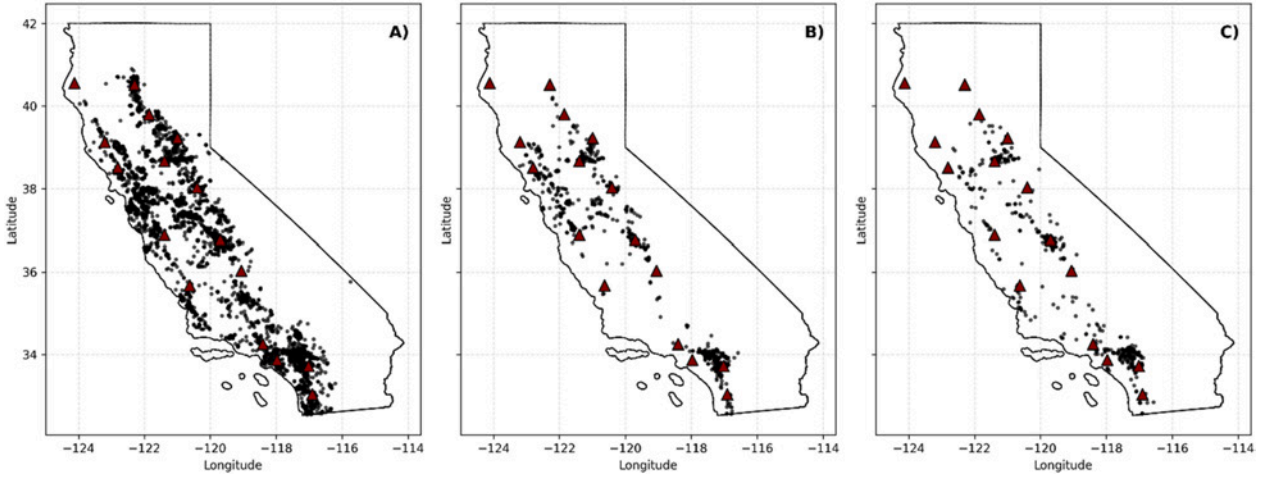

Fig. 3. Spatial distribution of fire response types and CAL FIRE airbases across California. Panels show (A) incidents with no aerial response, (B) incidents where CAL FIRE aircraft responded first, and (C) incidents where USFS aircraft responded first. Black points represent incident locations, and red triangles indicate airbase locations.

any single region.

3.4. NDVI results

Across all 7214 fires, standardized day-prior NDVI anomalies ranged from roughly −8 to +5, with most values falling between −2 and +2 and a slight tendency toward more negative anomalies during the core 2020 fire season (Figure A3). When grouped by event type, NDVI anomaly distributions for fires that received no aircraft and those that received an aerial response were broadly similar, with medians near zero and strongly overlapping interquartile ranges (Figure A4). In the Cox models, however, NDVI anomaly consistently had a negative and highly significant coefficient ($\beta \approx -0.10$, $p < 0.001$ in all three specifications; Table 3), indicating that, after accounting for fuel, weather, exposure, and distance-to-water covariates, increasingly positive NDVI anomalies were associated with lower estimated hazards of aircraft arrival and increasingly negative anomalies with higher hazards.

3.5. Cumulative incidence of first response

Cause-specific cumulative incidence functions (Fig. 4) show the probability of each agency being first to arrive over time. By 1440 min, the cumulative incidence reached approximately 0.12 for CAL FIRE and 0.09 for USFS. Confidence intervals (shaded bands) reflect uncertainty around each estimate.

3.6. Cox proportional hazards models

We estimated three Cox proportional hazards models: (1) an unstratified baseline model, (2) a model stratified by discovery time (Morning/Afternoon/Night), and (3) a model stratified by DPA region (Table 3). Schoenfeld residual diagnostics are provided in Figure A5, and robustness checks excluding covariate groups are shown in Table A6.

Across all three Cox model specifications, coefficient signs and magnitudes were consistent (Table 3). Maximum temperature, nearby population density, and human-modified landscape values had positive coefficients in every model, indicating higher estimated hazards of aircraft arrival when increased. NDVI anomaly, distance to water, and fuel moisture had negative coefficients across models. Slope, wind speed, and Burning Index showed coefficients near zero with no meaningful variation across specifications. Effect sizes for the major covariates were stable across Models 1–3, and no coefficient changed sign between models. The time-of-day–stratified model produced the lowest BIC value, indicating slightly better fit relative to the baseline and DPA-stratified models. Hazard ratios and confidence intervals from all three model specifications are shown in Figure A7.

The baseline survival functions for the DPA-stratified model (Model 3) differed across the three DPA groups (Fig. 5). STATE-managed fires ($n = 2006$) showed the steepest decline in survival probability over the 24-h window, indicating a higher baseline hazard of aircraft arrival under this stratification. Local DPAs ($n = 5088$) exhibited the slowest decline, maintaining the highest survival probabilities for most of the time range. Federal DPAs ($n = 120$) showed an intermediate trajectory, though the curve displayed more irregular step patterns compared to the other groups, reflecting the smaller sample size for federally managed fires. All curves steadily decreased, consistent with the accumulation of aircraft arrival events over the observation period.

4. Discussion

4.1. Response timing patterns and decision complexity

The cause-specific cumulative incidence curves rise steadily rather than showing an early step change, indicating that the probability of receiving an aircraft is relatively diffuse across the first 24 h during the IR phase (Fig. 4). If aircraft were commonly launched

Table 3
Coefficient estimates and standard errors from three Cox proportional hazards models examining factors associated with time to initial aircraft arrival on wildfires in California during the 2020 fire season. All models include the same covariates with Model 1 (unstratified), Model 2 (stratified by time of day), and Model 3 (stratified by DPA). Values represent log hazard coefficients; standard errors are in parentheses. Positive coefficients indicate factors associated with faster aircraft dispatch.

Variable	Model 1	Model 2 (Time strata)	Model 3 (DPA strata)
FM100	−0.074 (0.054)	−0.078 (0.054)	−0.064 (0.054)
NDVI anomaly	−0.100*** (0.024)	−0.101*** (0.024)	−0.099*** (0.024)
Slope	0.043 (0.031)	0.043 (0.031)	0.008 (0.035)
Distance to water	−0.060* (0.026)	−0.060* (0.026)	−0.037 (0.027)
Wind speed	−0.056 (0.041)	−0.056 (0.041)	−0.053 (0.040)
Burning Index	0.044 (0.058)	0.038 (0.058)	0.049 (0.058)
Max temp °F	0.448*** (0.038)	0.445*** (0.038)	0.464*** (0.038)
Global Human Mod	0.119* (0.051)	0.117* (0.051)	0.193*** (0.054)
Population	0.146** (0.047)	0.148** (0.047)	0.166** (0.048)
Num. Obs.	7214	7214	7214
BIC	25567.6	22441.0	23740.2

Notes: *$p < 0.05$; **$p < 0.01$; ***$p < 0.001$.

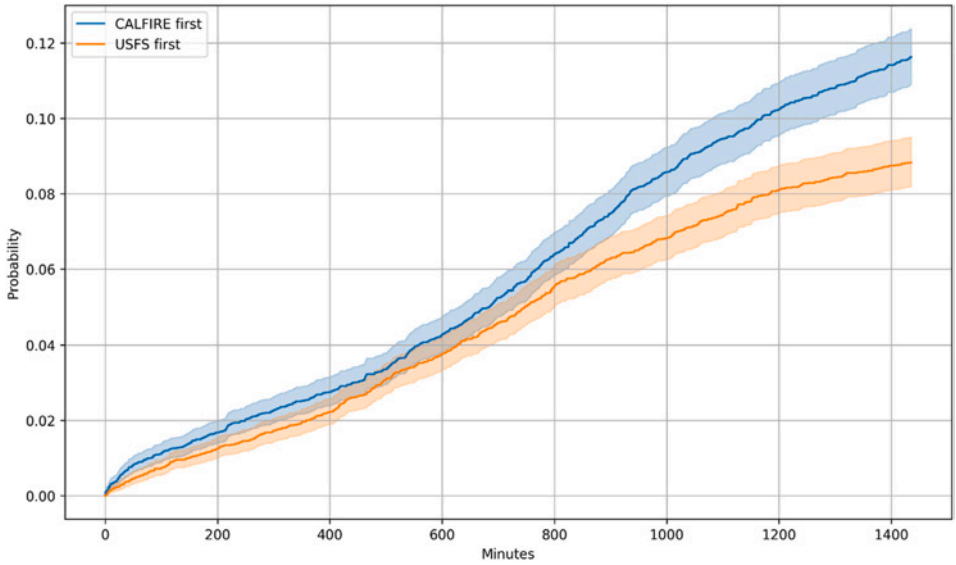

Fig. 4. CIFs estimated using the Aalen–Johansen method for initial aircraft response to wildfires in California during 2020. The blue line represents the probability over time that CAL FIRE is the first to respond; the orange line represents USFS. Shaded areas indicate 95% confidence intervals. Time is measured in minutes from fire discovery.

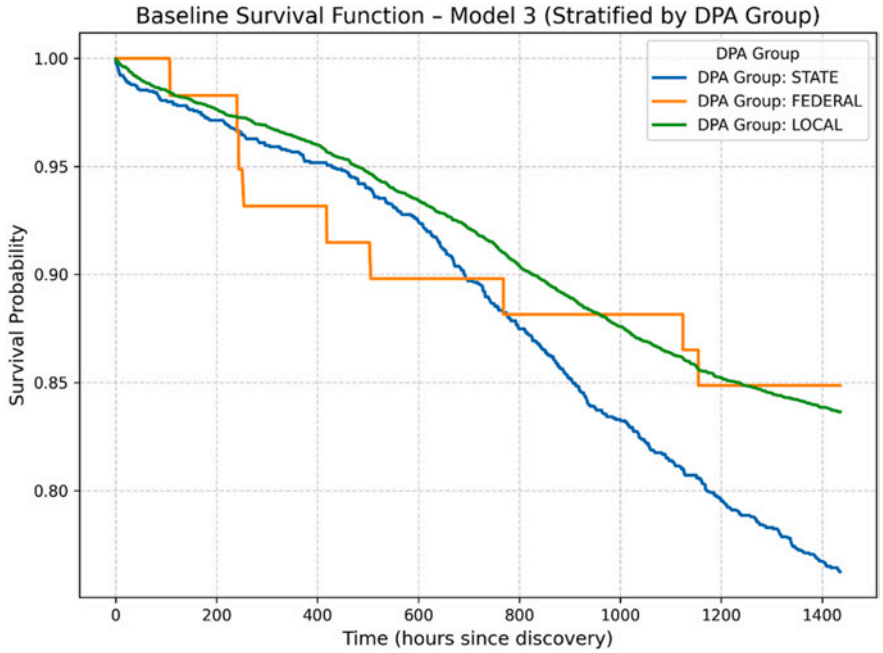

Fig. 5. Baseline survival functions from the DPA-stratified Cox model (Model 3). Curves show the estimated probability that no aircraft has arrived as a function of time since fire discovery for STATE, FEDERAL, and LOCAL Direct Protection Areas.

immediately at discovery, we would expect a sharp initial jump; instead, both agencies exhibit a near-linear accumulation, with only a small fraction of fires receiving aircraft in the first 20 min. This pattern is compatible with the absence of any single, predictable "clock" governing when aircraft are dispatched after a fire's discovery.

Responding to wildfire involves balancing multiple, sometimes competing priorities, including firefighter safety, suppression costs, public expectations, and the anticipated ecological outcomes of different response strategies, among others, which together shape when and how resources are deployed [51,52]. As a result, the timing of aerial response reflects the combined influence of fuel

moisture, weather, slope, access to water, proximity to people and infrastructure, and the evolving fire situation, factors that seldom align uniformly across incidents. Operationally, dispatch is also mediated by availability (what's on base, what's already committed), airspace and smoke constraints, and importantly, human decision-making under uncertainty [44]. That last element introduces real variability. Incident commanders weigh consequences, alternatives (ground attack, wait for IR/size-up), and risk thresholds differently, so two similar ignitions may lead to different call-up times. Together, these environmental, logistical, and human factors produce a broadly increasing, rather than front-loaded, arrival profile, with modest early responses and a persistent chance of first arrival throughout the IR window. Practically, this means that improving situational awareness, coordination, and decision support tools may do more to contribute to timely and effective aerial response than any single operational change alone.

4.2. Environmental drivers of aerial dispatch

Building on this broader understanding of how response decisions unfold, the modeled results further show that aircraft are more likely to be mobilized under conditions of higher temperatures, patterns observed in prior studies of aerial suppression behavior [30, 32]. This suggests weather, and more specifically hotter temperatures, may influence dispatch decisions. Wind speed, by contrast, had a small negative but statistically non-significant effect on the hazard of aircraft arrival, indicating no clear evidence that stronger winds systematically accelerate or delay aerial response in this dataset. This is consistent with operational practice, where incident commanders will still launch aircraft across a wide range of wind speeds when safety envelopes allow, even though higher winds are known to reduce drop effectiveness by increasing drift and making it harder for water or retardant to reach the target fuels [53]. Additionally, steep terrain has historically been a focal point for retardant operations; however, our models show no statistically significant association between slope and the hazard of aircraft arrival [30]. This may reflect either genuinely weak slope sensitivity in IR decision-making or the fact that ADS-B coverage is concentrated in lower-elevation terrain where slope variation is smaller and operational patterns differ from high-slope wilderness settings.

These same terrain- and weather-driven challenges also intersect with logistical considerations such as access to water. In our results, the distance to water term does not exhibit a consistently strong signal, suggesting that water availability may influence aviation use in some contexts but not uniformly across incidents. Several factors could explain this muted relationship. In remote areas where accessible water sources are scarce, longer ferry distances and fewer dip sites can constrain operations and shift reliance toward ground-based tactics [54]. Distance to water may also shape the type of aircraft used, the feasibility of placing water or retardant drops, and broader suppression strategies, but these influences may not manifest as a simple, statewide pattern.

Beyond logistics, distance to water is correlated with environmental characteristics that vary substantially across California's landscapes. Fires farther from water often occur in settings with lower fuel continuity or reduced vegetation productivity, where aerial support may offer limited marginal benefit compared to ground attack. For example [55], note that ecosystems with lower net primary productivity, common in arid regions distant from riparian areas, tend to have sparser or more discontinuous fuels, which constrain fire growth potential and may reduce the need for intensive aerial suppression. Thus, the weak statistical relationship observed here may reflect the combined influence of operational constraints, longer ferry distances, ecological gradients, and differences in fuel structure rather than a direct, statewide effect of water proximity alone.

4.3. Live fuel signals and NDVI anomalies

Across all three Cox models, the NDVI anomaly term is negative and highly significant, indicating that live-fuel conditions exert a consistent influence on whether aircraft are dispatched quickly. Because the anomaly was constructed so that negative values represent below-normal greenness for that location and month (drier, more stressed live fuels) and positive values represent greener-than-usual conditions, the negative coefficient means that fires igniting under more stressed vegetation are more likely to receive aircraft earlier. In standardized units, a one–standard deviation increase in the NDVI anomaly term (toward greener-than-expected vegetation) reduces the likelihood of aircraft arrival by roughly 10%, whereas a one–standard deviation shift toward more negative anomalies increases the likelihood of using aircraft. This pattern is consistent with prior work showing that NDVI anomalies and departures from “normal” greenness track live fuel moisture and elevated fire potential [34–36] and with recent efforts to incorporate improved live-fuel moisture representations into fire danger systems [38]. Together, these results suggest that incident commanders are more inclined to mobilize aircraft under conditions when live fuels appear unusually dry for the season, not just when background dead fuels are dry, and that NDVI-derived indicators provide information about response decisions beyond what is captured by FM100 or composite fire-danger indices alone. This emphasis on anomalously dry fuels aligns with broader evidence from the 2020 season that unusual fuel conditions contributed to concerns about late-season large-fire potential and shaped strategic planning for suppression capacity [56].

4.4. Human exposure and values at risk

While these environmental and logistical factors help explain where aircraft are less likely to be deployed, human and social factors appear equally important in determining where they are. Aviation deployments during initial response tend to intensify where high-value property is at stake [57]. Our model reproduces this pattern through positive coefficients on both the global human modification and population. Multiple empirical studies indicate that proximity to people and property is a strong driver of aerial-suppression

decisions. A nationwide analysis of large-air-tanker missions during 2010–2014 showed that aviation assets were disproportionately concentrated within about 10 km of the wildland–urban interface, where population density and infrastructure are highest [32]. A more detailed review of 2012 operations in Montana found the median distance from drop locations to mapped WUI values was only 2.8 mi, underscoring how protection of communities shapes deployment patterns [58]. Consistent with these case studies, the U.S. Forest Service's Aerial Firefighting Use and Effectiveness (AFUE) program reported that most drops across all aircraft types occurred on fires where values were threatened during the event, signaling that resource-at-risk considerations routinely influence aviation tasking at the national scale [59]. Taken together with our findings, these studies reinforce that aircraft are preferentially mobilized when fires threaten concentrated assets, whether homes or infrastructure, explaining the strong population-proximity signal in our hazard models.

4.5. Data coverage constraints and observational bias

While these results capture genuine operational behavior, they also reflect the spatial and technical constraints of ADS-B data. This limitation is particularly relevant for low-altitude helicopter operations and terrain-following flight typical of initial response, where line-of-sight reception may be reduced. Line-of-sight reception means that ground-based ADS-B networks provide denser coverage in populated corridors and lower-elevation valleys, especially the Central Valley and Sierra foothills, while reception drops off in remote, mountainous regions such as far-northern coastal California, the high Sierra, and the southeastern deserts. To avoid conflating absent detections with absent response, we excluded 1003 fires with no ADS-B messages within 5 km in 2020; however, this necessary filter shifts the analytic sample toward areas with robust sensor coverage, greater airbase density, and higher WUI exposure. Consequently, the estimated probabilities and timing of aerial response may be somewhat upward-biased relative to true statewide patterns, and differences between agencies may be muted if one agency more frequently serves wilderness and high-elevation terrain. Our findings should therefore be interpreted as describing IR activity that is observable via ADS-B, rather than representing all IR operations statewide. Future work could reduce these gaps by incorporating satellite-based ADS-B reception or by outfitting aircraft with onboard, internet-connected systems capable of relaying position data in real time.

4.6. Implications for aviation monitoring systems

Despite these coverage limitations, ADS-B nevertheless provides a uniquely comprehensive view of aerial activity compared with traditional data sources. Existing wildfire aviation studies have relied primarily on ATU drop logs, which are mandatory for federally contracted airtankers but not for state fleets such as CAL FIRE. As a result, analyses using only ATU data (e.g., Ref. [60,61]) omit substantial portions of aerial suppression performed by state and private aircraft. ADS-B addresses much of this limitation, because all transponder-equipped aircraft broadcast their position every second. Open networks like the OpenSky Network provide ownership-agnostic, continuous records of aircraft movement. Prior work has already shown that straightforward pattern-recognition methods applied to ADS-B tracks can identify CAL FIRE airtankers, map circling orbits over active fires, and reconstruct operational timelines without access to mission logs [18].

ADS-B's strengths stem from its open broadcast architecture; low-cost receivers can collect signals wherever line-of-sight exists, and community archives now contain billions of messages [62]. When integrated with incident records or the subset of federal ATU drops, these data support new spatial analyses of fleet utilization. Yet the system remains incomplete: coverage is uneven, mountainous terrain can obscure reception, and some aircraft still operate without broadcasting ADS-B even within mandated airspace. Advancing wildfire aviation research will therefore require hybrid data systems that merge terrestrial and satellite ADS-B, agency-specific telemetry, and emerging unmanned-aircraft sensors. Such integration would produce a more comprehensive and resilient picture of aerial firefighting activity and extend performance analyses beyond federal fleets to the state and local resources that increasingly shoulder IR responsibilities.

5. Conclusion

Fig. 3 shows that the spatial distribution of response types is broadly consistent across California, with no discernible geographic clustering that would indicate systematic spatial bias in whether CAL FIRE or the USFS responds first. Incidents with no aerial response, CAL FIRE–first responses, and USFS–first responses all occupy the same statewide footprint, which aligns with the fact that CAL FIRE airbases are strategically located to provide wide and relatively uniform coverage. Because the airbase network is intentionally designed to minimize spatial gaps, a strong geographic signature in response patterns is not expected. The violin plot (Figure A2) shows a slight tendency for incidents receiving an initial aerial response to occur at somewhat shorter distances from CAL FIRE airbases compared with no-response incidents. This weak proximity signal is operationally intuitive: closer fires are more likely to receive aircraft simply because travel times are shorter and aircraft can be committed more efficiently. Overall, proximity to airbases appears to play a modest role in shaping response likelihood and sequencing, but it does not produce a pronounced spatial pattern across the state.

The results of this study indicate a cooperative balance in aviation workload between CAL FIRE and the USFS, reflecting the intertwined responsibilities defined under California's Direct Protection Area agreements. Despite differences in fleet composition and mission scope, the expected response times for the two agencies are nearly identical within the ADS-B–observable portion of the state

(Figure A8). This similarity suggests that, operationally, both agencies are contributing comparably to IR aviation response during high-activity periods.

Workload patterns further reinforce this shared commitment. The seasonal activity curves for the two fleets exhibit a nearly unimodal, parallel structure, with both agencies showing a midsummer–early fall pulse in aircraft activity (Fig. 2). The similarity in these seasonal pulses indicates that both fleets scaled up and sustained aviation effort during the same fire-season periods, consistent with coordinated IR responsibilities. Spatial patterns also suggest a roughly even division of effort: the distribution of incidents first reached by each agency (Fig. 3) shows substantial geographic overlap, rather than a clear partitioning of responsibility.

This balanced pattern of effort and engagement aligns with prior work documenting shared federal–state response structures and cooperative aviation management under DPA agreements and closest-resource dispatch protocols National Interagency Coordination Center [1,5]. It is also consistent with findings from Stonesifer et al. [32], who showed that large airtanker use is requested at the incident level through a national dispatch system and is concentrated near populated areas, indicating that deployments are driven by operational needs and proximity to values at risk rather than purely by jurisdictional boundaries. Together, these results suggest that the combined CAL FIRE and USFS aviation systems operate less as two separate fleets than as a jointly involved suppression network responding to similar environmental triggers and workload pressures.

This study demonstrates that ADS-B's global, second-by-second telemetry provides a uniquely comprehensive lens on wildfire aviation use, allowing us to quantify when, where, and under what conditions CAL FIRE and USFS aircraft launch during initial response, something that has not been possible with traditional, agency-specific records. By linking aircraft trajectories with survival analysis, we show how terrain, weather, water access, and values-at-risk shape deployment timing and reveal patterns that were previously obscured by fragmented reporting systems. Rather than directly comparing agencies, our analysis illustrates how a unified, ownership-agnostic data stream can illustrate the broader operational environment in which both systems operate. As ADS-B continues to expand, further integration with federal and state tracking systems, shared data protocols, and more consistent coverage will strengthen its potential as the foundation for real-time coordination, performance assessment, and long-term planning. Together, these advances point toward a future in which a consolidated monitoring architecture supports more transparent, equitable, and strategically informed use of aviation resources during wildfire response.

CRediT authorship contribution statement

Shayne Magstadt: Writing – original draft, Visualization, Methodology, Investigation, Formal analysis, Data curation, Conceptualization. **Erin J. Belval:** Writing – review & editing, Supervision, Resources, Methodology, Conceptualization. **Bradley M. Pietruszka:** Writing – review & editing, Validation, Supervision, Formal analysis, Conceptualization. **Yu Wei:** Writing – review & editing, Supervision, Investigation, Conceptualization. **Christopher D. O'Connor:** Writing – review & editing, Resources, Funding acquisition.

Funding acknowledgement

This work was supported by the United States Department of Agriculture, Forest Service, Rocky Mountain Research Station under Challenge Cost Share Agreement No. 22-CS-11221636-189 with Colorado State University.

Funding statement

Funding was provided through a Challenge Cost Share Agreement between Colorado State University and the U.S. Forest Service, Rocky Mountain Research Station (Agreement No. 22-CS-11221636-189).

Declaration of competing interest

The authors declare that they have no known competing financial interests or personal relationships that could have appeared to influence the work reported in this paper.

Acknowledgements

The author would like to thank Lucila Corro for her invaluable contributions to the conceptual framing of this study, as well as for her support during the original drafting process. Her thoughtful editing, critical feedback, and continued engagement throughout the development of the manuscript substantially strengthened the clarity, structure, and overall direction of this work. Without her support, this paper would not have been possible.

Appendix

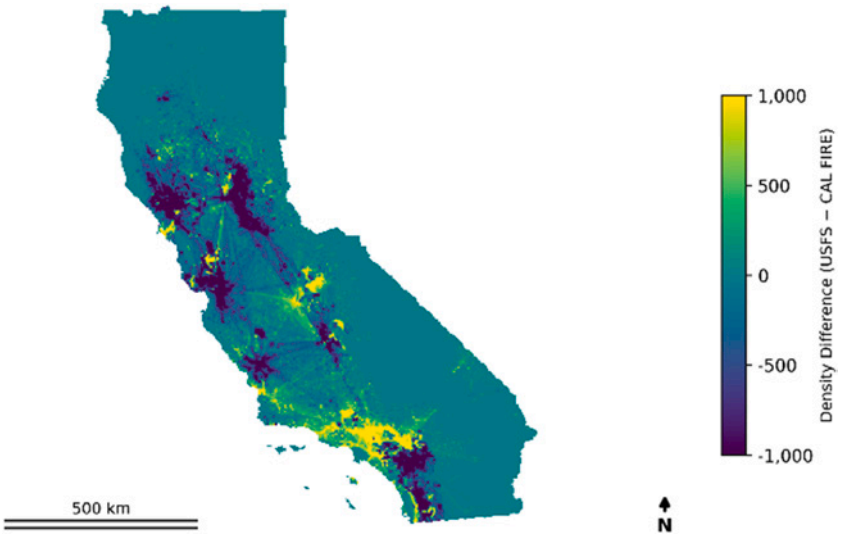

Fig. A1. Difference in ADS-B–derived aircraft density between USFS and CAL FIRE aircraft across California during the 2020 fire season. Values represent USFS minus CAL FIRE cumulative aircraft-seconds per 3-km grid cell, with bright yellow areas indicating more frequent USFS use and dark purple areas indicating more frequent CAL FIRE use.

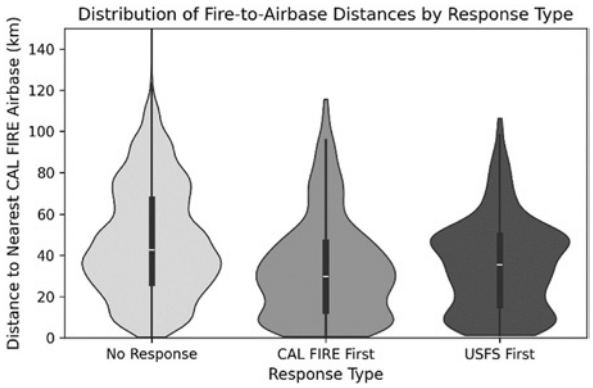

Fig. A2. Violin plots showing distances from fires to the nearest CAL FIRE airbase, grouped by response type (No Response, CAL FIRE first, USFS first).

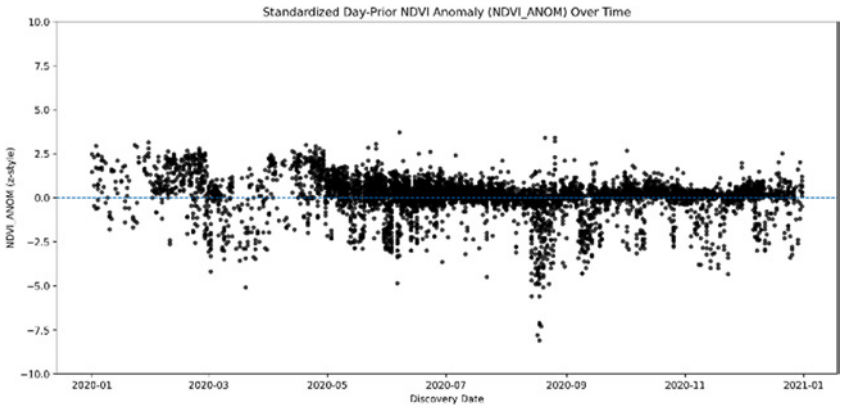

Fig. A3. Standardized day-prior NDVI anomalies for all 2020 fires, showing departures from typical monthly greenness conditions over the fire season.

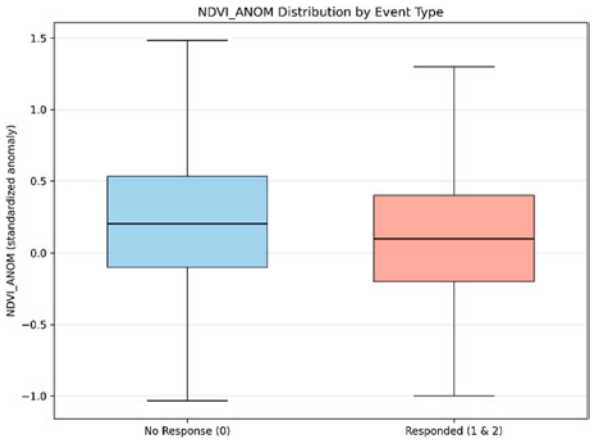

Fig. A4. Boxplots comparing standardized NDVI anomalies for fires with no aerial response versus those that received an initial aircraft response.

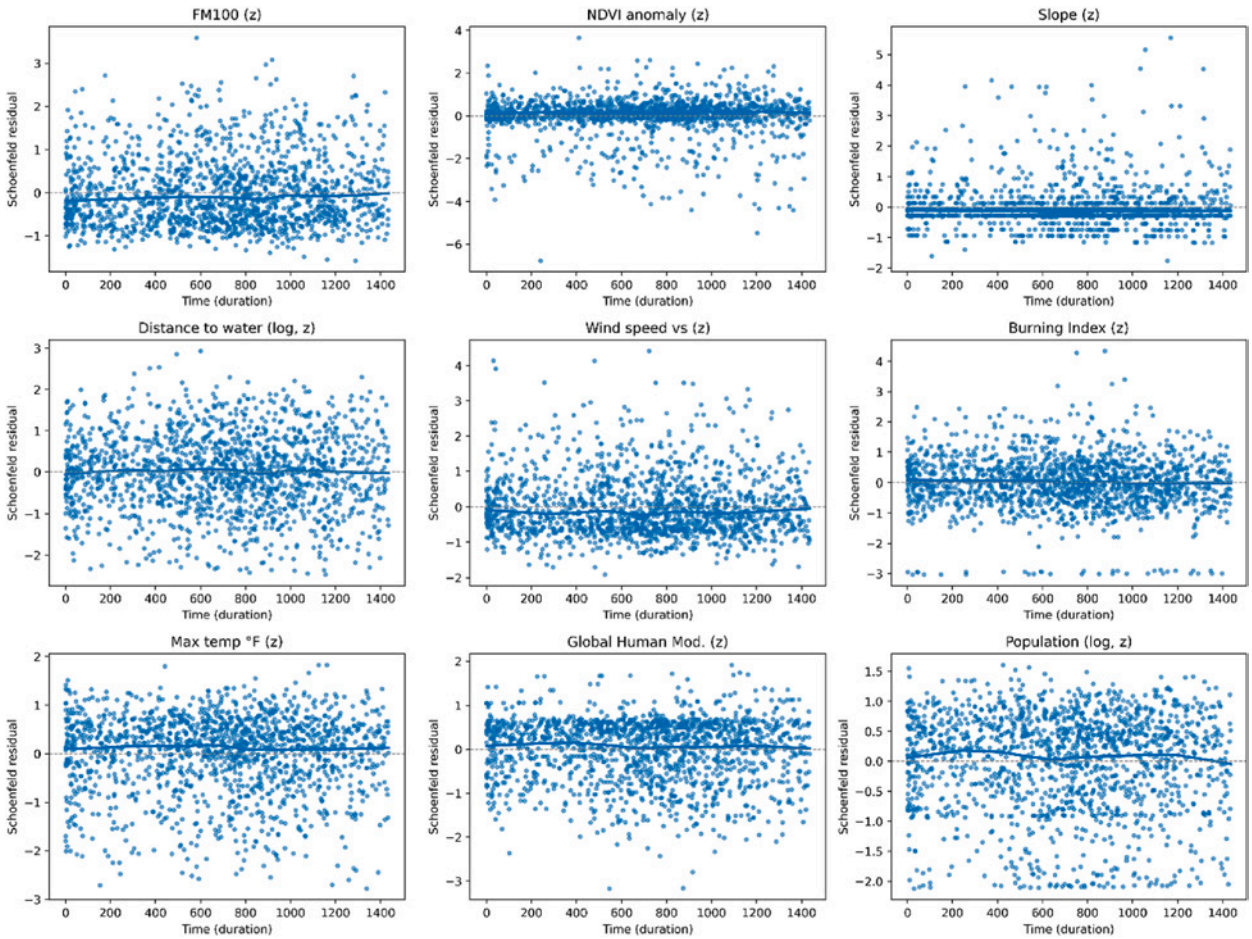

Fig. A5. Schoenfeld residuals for model 1 used to assess the proportional hazards assumption of the dataset.

We evaluated the proportional hazards assumption of the Cox regression models using Schoenfeld residuals, visualized via the CoxPHFitter function in the lifelines library. These plots assess whether residuals remain independent of time, a key requirement for

the validity of proportional hazards modeling. As shown in Figure A5, most covariates exhibit residuals that fluctuate randomly around zero, suggesting reasonable adherence to the assumption. Although formal statistical tests flagged minor violations for some covariates, these are likely artifacts of the large sample size or the continuous nature of the predictors rather than substantive departures from proportionality [63]. Given the stability of effect estimates across stratified model specifications and the lack of strong temporal patterns in residuals, we interpret the models as appropriately specified for estimating how landscape, weather, and exposure factors influence aircraft dispatch timing during the initial response phase.

Table A6
Robustness checks for Cox PH regression results.

Variable	Full	No_Slope	No_Pop	No_Fuel	No_Weather
Global Human Mod	0.892*** (0.193)	0.799*** (0.178)	Not included	0.861*** (0.192)	0.986*** (0.193)
NDVI anomaly	−0.097*** (0.025)	−0.098*** (0.025)	−0.090*** (0.025)	Not included	−0.108*** (0.025)
Population	0.006† (0.004)	0.007† (0.004)	Not included	0.006 (0.004)	0.007† (0.004)
Slope	0.009 (0.007)	Not included	−0.015* (0.006)	0.009 (0.007)	0.003 (0.007)
Burning Index	0.003 (0.003)	0.003 (0.003)	0.004 (0.003)	0.006** (0.002)	Not included
Distance to water	−0.034** (0.011)	−0.035** (0.011)	−0.039*** (0.011)	−0.036** (0.011)	−0.031** (0.011)
FM100	−0.021 (0.015)	−0.021 (0.015)	−0.003 (0.015)	Not included	−0.109*** (0.009)
Max Temp °F	0.034*** (0.003)	0.034*** (0.003)	0.035*** (0.003)	0.036*** (0.003)	Not included
Wind speed	−0.041 (0.027)	−0.041 (0.027)	−0.056* (0.027)	−0.054* (0.024)	Not included
Num.Obs.	7214	7214	7214	7214	7214
BIC	25569.5	25562.2	25612.7	25567.4	25703.1
Notes	†p < 0.10, *p < 0.05, **p < 0.01, ***p < 0.001. Standard errors in parentheses.				

To evaluate the robustness of our findings, we estimated several alternative model specifications presented in Table A6. The first column reproduces our full model used in the main analysis. Each subsequent column systematically excludes a set of related covariates, slope, population, fuel, and weather, to assess the sensitivity of our estimates to specific predictor domains.

Overall, the direction and significance of most coefficients remain stable across specifications, particularly for human modification and max temperature, indicating strong and consistent effects. Notably, removing weather variables slightly attenuates some associations and increases the BIC, suggesting that weather contributes meaningfully to model fit. Dropping slope or population-related terms had minimal impact on other coefficients, while the removal of fuel variables slightly shifted the estimates of related predictors. These results support the robustness of our core findings, with minor variations in magnitude attributable to shared variance across covariates rather than fundamental instability in the model.

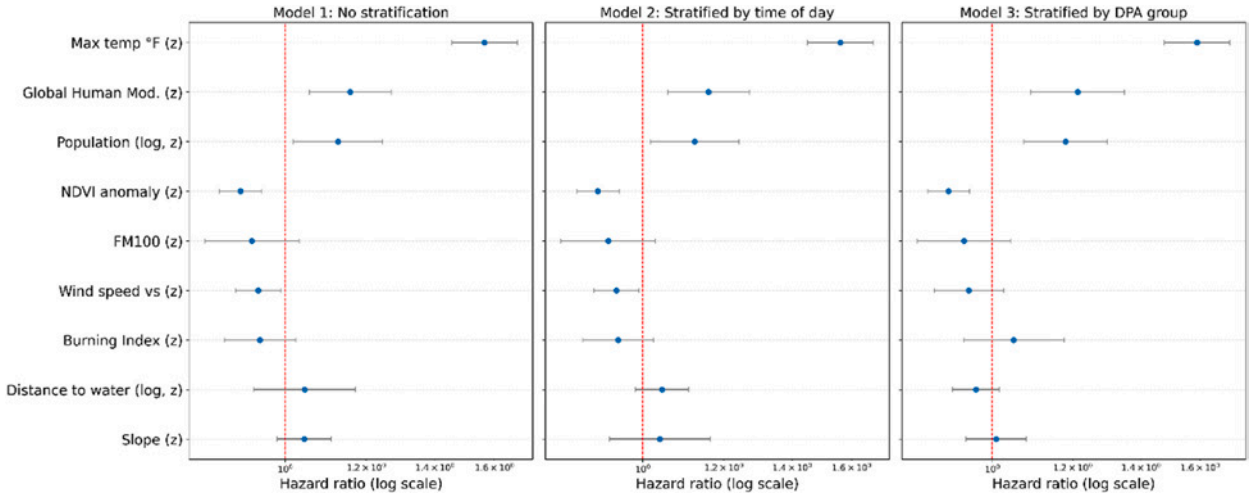

Fig. A7. Hazard ratios and 95% confidence intervals from three Cox proportional hazards models evaluating factors influencing the timing of initial aircraft dispatch. Each panel corresponds to a different model specification: (left) Model 1 with no stratification, (center) Model 2 stratified by time of day (morning, afternoon, night), and (right) Model 3 stratified by DPA. The red dashed vertical line at HR = 1 denotes the null effect.

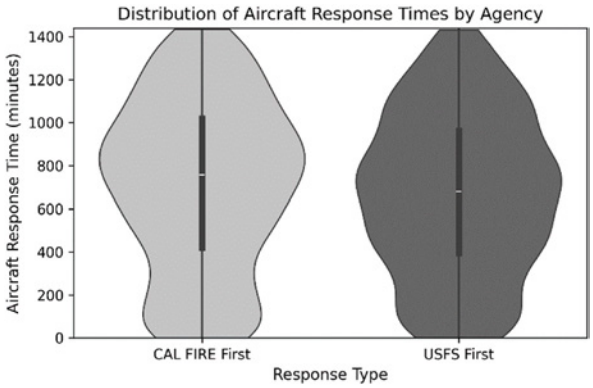

Fig. A8. Violin plots comparing aircraft response times for fires first reached by CAL FIRE versus USFS during the 2020 season.

Data availability

The authors do not have permission to share data.

References

[1] U.S. Forest Service, Aviation strategic plan 2022-2026, Available at: https://www.fs.usda.gov/sites/default/files/2023-06/Aviation-Strategic-Plan22-26.pdf, 2023.
[2] CAL FIRE, Aviation Program, California Department of Forestry and Fire Protection (CAL FIRE), 2025. Available at: https://www.fire.ca.gov/what-we-do/fire-protection/aviation-program.
[3] K. Pimlott, J. Laird, E.G. Brown Jr, Wildfire activity statistics, California Depart. Forest. Fire Protect. Offic. StateFire Marshal (2015) 1–45.
[4] U.S. Forest Service, CY2020 U.S. Forest Service Aviation Annual Report, U.S. Department of Agriculture, Forest Service, 2021. Available at: https://www.fs.usda.gov/sites/default/files/2021-06/CY2020_USFSAviationReport_Final_1.pdf.
[5] National Interagency Coordination Center (NICC), National Interagency Mobilization Guide, 2023rd edn, National Interagency Fire Center, 2023. Boise, ID, https://www.nifc.gov/sites/default/files/NICC/3-Logistics/Reference%20Documents/Mob%20Guide/Mobilization_Guide.pdf.
[6] H.D. Safford, A.K. Paulson, Z.L. Steel, D.J.N. Young, R.B. Wayman, The 2020 California fire season: a year like no other, a return to the past or a harbinger of the future? Global Ecol. Biogeogr. 31 (10) (2022) 2005–2025, https://doi.org/10.1111/geb.13498.
[7] T.W. Porter, W. Crowfoot, G. Newsom, Wildfire Activity Statistics, California Department of Forestry and Fire Protection, Sacramento, CA, USA, 2020, p. 46.
[8] J. Keeley, A. Syphard, Large California wildfires: 2020 fires in historical context, Fire Ecol. 17 (2021) 22.
[9] U.S. Forest Service, Interagency Aviation Information Bulletin 2021-08, 2021. Available at: https://www.fs.usda.gov/sites/default/files/2022-06/iaib-2021-08.pdf.
[10] M. Varga, Z.A. Polgár, H. Hedeşiu, ADS-B based real-time air traffic monitoring system, in: 2015 38th International Conference on Telecommunications and Signal Processing (TSP), IEEE, 2015, pp. 215–219.
[11] B.S. Ali, System specifications for developing an Automatic Dependent Surveillance-Broadcast (ADS-B) monitoring system, Int. J. Critical Infrastruct. Protect. 15 (2016) 40–46.
[12] M. Leonardi, ADS-B anomalies and intrusions detection by sensor clocks tracking, IEEE Trans. Aero. Electron. Syst. 55 (5) (2018) 2370–2381.
[13] Federal Aviation Administration, Electronic code of federal regulations: 14 CFR § 91.225 - Automatic Dependent Surveillance-Broadcast (ADS-B) Out equipment and use, Available at: https://www.ecfr.gov/current/title-14/chapter-I/subchapter-F/part-91/subpart-C/section-91.225, 2020. (Accessed 19 August 2023).
[14] L. Martin, Y. Arbab, L. Roberts, J. Mercer, C. Walter, W. McCarty, C. Sheehe, Developing an unmanned aircraft system pilot kit (UASP-kit) for wildland fire UAS operators, in: AIAA AVIATION 2022 Forum, 2022, p. 4003.
[15] D.L. Bakowski, L. Martin, G. Dustin, C. Mariano, Incorporating UAS traffic management into wildland firefighting operations: initial findings of subject matter expert interviews, in: 2024 AIAA DATC/IEEE 43rd Digital Avionics Systems Conference (DASC), IEEE, 2024, pp. 1–10.
[16] A. Struminska, A. Filippone, Flight performance analysis of aerial fire fighting, Aeronaut. J. (2024) 1–29.
[17] M. Schäfer, M. Strohmeier, V. Lenders, I. Martinovic, M. Wilhelm, Bringing up OpenSky: a large-scale ADS-B sensor network for research, in: IPSN-14 Proceedings of the 13th International Symposium on Information Processing in Sensor Networks, IEEE, 2014, pp. 83–94.
[18] X. Olive, J. Sun, A. Lafage, L. Basora, Detecting events in aircraft trajectories: rule-based and data-driven approaches, in: Proceedings, MDPI, 2020, p. 8.
[19] S. Magstadt, Y. Wei, B.M. Pietruszka, D.E. Calkin, A deep learning approach for predicting aerial suppressant drops in wildland firefighting using automatic dependent surveillance–broadcast data, Fire 7 (11) (2024) 380.
[20] Federal Aviation Administration, Aircraft inquiry: N-number registry, Available at: https://registry.faa.gov/aircraftinquiry/search/nnumberinquiry, 2020.
[21] J. Sun, H. Vû, J. Ellerbroek, J.M. Hoekstra, pyModeS: decoding mode-S surveillance data for open air transportation research, IEEE Trans. Intell. Transport. Syst. (2019), https://doi.org/10.1109/TITS.2019.2914770 [Preprint].
[22] NASA JPL, NASADEM merged DEM global 1 arc-second V001. https://doi.org/10.5067/MEASUREs/NASADEM/NASADEM_HGT.001, 2020.
[23] M. Strohmeier, X. Olive, J. Lübbe, M. Schäfer, V. Lenders, Crowdsourced air traffic data from the OpenSky Network 2019–2020, Earth Syst. Sci. Data 13 (2) (2021) 357–366.
[24] K.C. Short, Spatial Wildfire Occurrence Data for the United States, 2022, pp. 1992–2020 [FPA_FOD_20221014]'.
[25] Congressional Research Service, Federal interagency wildfire response framework, IF12384. Library of Congress. Available at: https://www.congress.gov/crs_external_products/IF/PDF/IF12384/IF12384.3.pdf, 2023.
[26] O.O. Aalen, S. Johansen, An empirical transition matrix for non-homogeneous Markov chains based on censored observations, Scand. J. Stat. (1978) 141–150.
[27] D.R. Cox, Regression models and life-tables, J. Roy. Stat. Soc. B 34 (2) (1972) 187–202.
[28] N. Breslow, Covariance analysis of censored survival data, Biometrics (1974) 89–99.
[29] D. Schoenfeld, Partial residuals for the proportional hazards regression model, Biometrika 69 (1) (1982) 239–241.
[30] M.P. Thompson, C.J. Lauer, D.E. Calkin, J.D. Rieck, C.S. Stonesifer, M.S. Hand, Wildfire response performance measurement: current and future directions, Fire 1 (2) (2018) 21.

[31] K. Reinke, S. Jones, S. Ramsey, N. Trihantoro, Utility of Himawari-8 Observations to Explore Aerial Suppression Activities, CSIRO and Bushfire and Natural Hazards CRC, Melbourne, 2021. Research Report.
[32] C.S. Stonesifer, D.E. Calkin, M.P. Thompson, K.D. Stockmann, Fighting fire in the heat of the day: an analysis of operational and environmental conditions of use for large airtankers in United States fire suppression, Int. J. Wildland Fire 25 (5) (2016) 520–533.
[33] Y. Pourmohamad, J.T. Abatzoglou, E.J. Belval, E. Fleishman, K. Short, M.C. Reeves, N. Nauslar, P.E. Higuera, E. Henderson, S. Ball, et al., Physical, social, and biological attributes for improved understanding and prediction of wildfires: FPA FOD-attributes dataset, Earth Syst. Sci. Data Discuss. 2023 (2023) 1–29.
[34] R.E. Burgan, Using NDVI to Assess Departure from Average Greenness and its Relation to Fire Business, US Department of Agriculture, Forest Service, Intermountain Research Station, 1996.
[35] E. Chuvieco, D. Cocero, D. Riano, P. Martin, J. Martınez-Vega, J. De La Riva, F. Pérez, Combining NDVI and surface temperature for the estimation of live fuel moisture content in forest fire danger rating, Rem. Sens. Environ. 92 (3) (2004) 322–331.
[36] B. Sall, M.W. Jenkins, J. Pushnik, Retrospective analysis of two northern California wild-land fires via Landsat five satellite imagery and Normalized Difference Vegetation Index (NDVI), Open J. Ecol. 3 (4) (2013) 311–323, https://doi.org/10.4236/oje.2013.34036.
[37] P.L. Andrews, D.O. Loftsgaarden, L.S. Bradshaw, Evaluation of fire danger rating indexes using logistic regression and percentile analysis, Int. J. Wildland Fire 12 (2) (2003) 213–226.
[38] W.M. Jolly, P.H. Freeborn, L.S. Bradshaw, J. Wallace, S. Brittain, Modernizing the US National Fire Danger Rating System (version 4): simplified fuel models and improved live and dead fuel moisture calculations, Environ. Model. Software 181 (2024) 106181.
[39] R.C. Rothermel, Modeling Moisture Content of Fine Dead Wildland Fuels: Input to the BEHAVE Fire Prediction System, vol. 359, United States Department of Agriculture, Forest Service, Intermountain Research Station, 1986.
[40] M. Wheatley, B.M. Wotton, D.G. Woolford, D.L. Martell, J.M. Johnston, Modelling decisions concerning the dispatch of airtankers for initial attack on forest fires in Ontario, Canada, Can. J. For. Res. 53 (4) (2022) 217–233.
[41] W.G. Page, B.W. Butler, Fuel and topographic influences on wildland firefighter burnover fatalities in Southern California, Int. J. Wildland Fire 27 (3) (2018) 141–154.
[42] J.T. Abatzoglou, Development of gridded surface meteorological data for ecological applications and modelling, Int. J. Climatol. 33 (1) (2013) 121–131.
[43] H. Simpson, M. Storey, M. Plucinski, O. Price, Investigating the Suitability of Aviation Tracking Data for Use in Bushfire Suppression Effectiveness Research – Black Summer Final Report, Bushfire and Natural Hazards CRC, 2022. Technical Report 725.2022, https://www.naturalhazards.com.au/sites/default/files/2022-04/Investigating%20the%20suitability%20of%20aviation%20tracking%20data%20for%20use%20in%20bushfire%20suppression%20effectiveness%20research_Black%20Summer%20final%20report.pdf.
[44] M.P. Thompson, D.E. Calkin, Uncertainty and risk in wildland fire management: a review, J. Environ. Manag. 92 (8) (2011) 1895–1909.
[45] M. Plucinski, Review of Aerial Suppression Effectiveness Research Literature, 2025.
[46] E. Vermote, NOAA climate data record (CDR) of AVHRR normalized difference vegetation index (NDVI), version 5, NOAA Nation. Center. Environm. Inform. 10 (2019). V5ZG6QH9.
[47] M.G. Rollins, LANDFIRE: a nationally consistent vegetation, wildland fire, and fuel assessment, Int. J. Wildland Fire 18 (3) (2009) 235–249.
[48] California Department of Fish and Wildlife, California Lakes, California Department of Fish and Wildlife, 2025. Available at: https://gis.data.ca.gov/datasets/CDFW::california-lakes-1.
[49] C.M. Kennedy, J.R. Oakleaf, D.M. Theobald, S. Baruch-Mordo, J. Kiesecker, Managing the middle: a shift in conservation priorities based on the global human modification gradient, Glob. Change Biol. 25 (3) (2019) 811–826.
[50] WorldPop and CIESIN, Global High-Resolution Population Density (1\,km) – UN Adjusted: United States of America, 2020, WorldPop, University of Southampton, 2018, https://doi.org/10.5258/SOTON/WP00674.
[51] M.A. Taber, L.M. Elenz, P.G. Langowski, Decision Making for Wildfires: A Guide for Applying a Risk Management Process at the Incident Level vol. 59, US Department of Agriculture, Forest Service, Rocky Mountain Research Station, Fort Collins, CO, 2013, p. 298. Gen. Tech. Rep. RMRS-GTR-298WWW.
[52] S.D. Fillmore, S. McCaffrey, R. Bean, A.M. Evans, J. Iniguez, A. Thode, A.M. Smith, M.P. Thompson, Factors influencing wildfire management decisions after the 2009 US federal policy update, Int. J. Wildland Fire 33 (1) (2024).
[53] L. Fogarty, A. Slijepcevic, The influence of wind speed on the effectiveness of aerial fire suppression, Fire Technol. Transf. Note (17) (1998) [Preprint].
[54] E.G. Keating, A.R. Morral, C.C. Price, D. Woods, D.M. Norton, C. Panis, E. Saltzman, R. Sanchez, Air Attack against Wildfires: Understanding US Forest Service Requirements for Large Aircraft, Rand Corporation, 2012.
[55] J.R. McNorton, F. Di Giuseppe, A global fuel characteristic model and dataset for wildfire prediction, Biogeosciences 21 (1) (2024) 279–300.
[56] E.J. Belval, K.C. Short, C.S. Stonesifer, D.E. Calkin, A historical perspective to inform strategic planning for 2020 end-of-year wildland fire response efforts, Fire 5 (2) (2022) 35.
[57] J. Bayham, J.K. Yoder, Resource allocation under fire, Land Econ. 96 (1) (2020) 92–110.
[58] C.S. Stonesifer, M.P. Thompson, D. Calkin, C.W. McHugh, Characterizing large airtanker use in United States fire management, in: Robert E. Keane, Matt Jolly, Russell Parsons, Karin Riley (Eds.), Proceedings of the Large Wildland Fires Conference; May 19-23, 2014; Missoula, MT. Proc. RMRS-P-73, US Department of Agriculture, Forest Service, Rocky Mountain Research Station, Fort Collins, CO, 2015, pp. 314–316.
[59] U.S. Department of Agriculture, Forest Service, Aerial Firefighting Use and Effectiveness (AFUE) Report, Department of Agriculture, Washington, D.C.: U.S, 2020. Available at: URL if available.
[60] C. Stonesifer, C. Bryan, J. Bayham, D. Calkin, E. Belval, Firefighting aircraft: understanding current practices to shape future response in a changing world, Environ. Sci. Proc. 17 (1) (2022) 50.
[61] J. Bayham, C. Bryan, The economics of wildland firefighting aviation procurement and effectiveness, West. Econ. Forum (2023) 43–52.
[62] M. Schafer, M. Strohmeier, M. Smith, M. Fuchs, R. Pinheiro, V. Lenders, I. Martinovic, OpenSky report 2016: facts and figures on SSR mode S and ADS-B usage, in: 2016 IEEE/AIAA 35th Digital Avionics Systems Conference (DASC), IEEE, 2016, pp. 1–9.
[63] P.M. Grambsch, T.M. Therneau, Proportional hazards tests and diagnostics based on weighted residuals, Biometrika 81 (3) (1994) 515–526.